ICCSPA20 1570624957

Image Classification in Microwave Tomography using a Parametric Intensity Model

Mohanad Alkhodari, Amer Zakaria, and Nasser Qaddoumi
Department of Electrical Engineering, American University of Sharjah
PO Box 26666, Sharjah, UAE

***Abstract*—A study is conducted to investigate the use of a parametric intensity model for the process of image classification in biomedical microwave tomography (MWT). This process allows for extracting structural information about an object-of-interest (OI), which can be incorporated as prior information in an inversion algorithm. The parametric intensity model is based on a supervised Gaussian probabilistic model. The generated intensity model is used to classify three cross-sectional MWT images of human lower leg models. The classification is based on a Bayesian decision classifier. The resulting segments are used to extract structural information about the legs' contour.**

***Index Terms*—microwave tomography, parametric intensity model, Gaussian probability, Bayesian decision classifier, finite-element method, contrast source inversion.**

I. Introduction

Microwave Tomography (MWT) has been emerging as a promising imaging modality for biomedical applications. It got several advantages over other imaging modalities such as utilizing safe low-power non-ionizing electromagnetic (EM) radiation, being user-friendly, and having a low overall equipment cost.

In biomedical MWT, a human organ, which is the object-of-interest (OI), is interrogated with EM waves from surrounding transmitting antennas. Based on the tissue layers within the OI as well as the coupling medium surrounding it, electric fields with varying strength are scattered. These fields are measured at several receivers around the OI and are utilized as inputs for an inversion algorithm. The algorithm outputs images that estimates the bulk electrical properties within the human organ. These properties are the relative permittivity and the effective conductivity [1].

The enhancement of the reconstructed images quality has been a wide interest for researchers in this field. An effective method to improve these image is by incorporating prior information about the OI within the inversion algorithm. Such prior information include the outermost contour of the human organ and/or the location and properties of bulk tissues within the organ like fat, skin, and muscle tissues. To include this information, they need to be extracted first. This has been done via using virtual antennas [2], by incorporating other imaging modalities such as ultrasound [3], or manually from blind reconstructions [4]; blind reconstructions are the output images of an inversion algorithm if no prior information is provided.

In this paper, a method to estimate the prior information of the OI using a parametric intensity model is presented. Using the proposed technique, blind reconstructions are classified using the generated intensity model to extract structural information about different tissues within the OI. Then, the extracted information are to estimate the OI's outermost boundary, which can be used as prior information in the reconstruction process.

II. Forward and Inverse Simulations

Synthetic numerical data need to be generated using a forward solver to test the techniques presented in this paper. The solver utilized herein is an in-house two-dimensional (2D) finite-element method (FEM) algorithm [5].

Further, a 2D model of a human leg is created using a Magnetic Resonance Imaging (MRI) cross-sectional image shown in Fig. 1(a) [6]. The MRI image is imported to MATLAB, where the points corresponding to each tissue layer (skin, fat, muscle, and bones) are extracted and exported to GMSH [7]. GMSH uses the extracted points to create a 2D FE mesh shown in Fig. 1(b).

Next, several parameters are selected for the forward solver: (*i*) 0.8 GHz operating frequency, (*ii*) twenty-four transmitters and receivers co-located and distributed equally on a circle of radius 15 cm surrounding the OI, and (*iii*) 80:20 glycerin/water coupling matching medium with a relative complex permittivity of $26 - j18$ [8]. In regard to the relative complex permittivity values for different tissues in the model, they are: $42 - j18.8$ for skin, $11 - j2.3$ for fat, $55 - j20.5$ for muscle and $13 - j3$ for bones.

The generated synthetic data are inverted using multiplicatively-regularized finite-element contrast source inversion (MR-FEMCSI) technique [5]. For the inversion algorithm, the imaging domain is a circular region of radius 14 cm. The reconstruction of the OI's relative permittivity

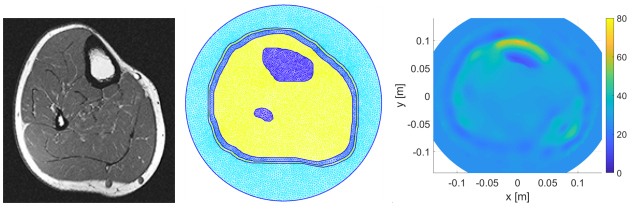

(a) MRI Image (b) FE Model (c) Reconstruction

Fig. 1. The forward model and inversion algorithm reconstruction: (a) MRI image [6], (b) 2D FE model, (c) relative permittivity reconstruction

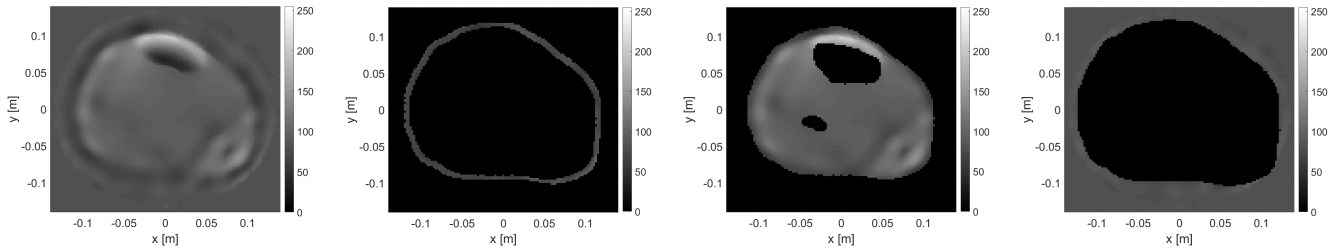

(a) Blind Reconstruction (b) Fat Tissue (c) Muscle Tissue (d) Matching Medium

Fig. 2. The bulk tissue regions extracted from the blind relative permittivity reconstructions: (a) blind reconstruction, (b) extracted fat tissue, (c) extracted muscle tissue, (d) extracted coupling medium.

is shown in Fig. 1(c). Further details about the forward and inversion simulations can be found in [9], [10].

III. Parametric Intensity Model

Prior structural information about the OI are extracted by generating a parametric intensity model for the blind relative permittivity reconstruction. The objective of generating this model is to assist in describing bulk objects in images.

A parametric intensity model can be expressed as a Gaussian, exponential, or Bernoulli probabilistic models [11]. In this paper, the selected model is the supervised Gaussian model, whose probability density function is given as,

$$p(q|k) = \frac{1}{\sqrt{2\pi\sigma_k^2}} e^{-\frac{(q-\mu_k)^2}{2\sigma_k^2}}. \quad (1)$$

Here $p(q|k)$ is the class-conditional probability density function or the *likelihood function* of each data point (or pixel) q within an image. The data point is sometimes referred to as a feature, which here is the relative permittivity value (or color intensity). As for k, it is a bulk region index. Furthermore, the mean and variance of the values within region k are, respectively, μ_k and σ_k^2. The model is considered supervised because training data are used to estimate the probabilities [11]. In this paper, the training data are the fat, muscle, and coupling medium regions obtained from the actual MRI-based FE model.

To calculate the parametric intensity model, the first step is to convert the reconstructed image from FEM-CSI to a gray-scaled image, whose range is from 0 to 255 as shown in Fig. 2(a). Next, the intensity values representing different tissues are extracted from the reconstructed blind image by masking bulk regions obtained from the original MRI-based FE model to the blind image. The extracted regions $k = \{1, 2, 3\}$ are,

1) Low permittivity fat-tissue region (Fig. 2(b)).
2) High permittivity muscle-tissue region (Fig. 2(c)).
3) Glycerin/Water coupling medium region (Fig. 2(d)).

After regions are extracted from the reconstructed image, the mean and variance for the values within each region are calculated. Moreover, the mean and variance of the relative permittivity for each region are given in Table I. In this table, the values between brackets are the gray-scaled intensity values. It should be noted that the bones regions are not extracted due to their poor reconstruction in terms of shape, location, and electrical properties.

TABLE I
Mean and Variance for the Parametric Intensity Model

Region	μ_k	σ_k^2
Fat-Tissue	13.49 (72.36)	8.72 (46.76)
Muscle-Tissue	20.96 (97.17)	75.58 (350.40)
Coupling Medium	17.62 (81.71)	1.59 (7.38)

Next, to generate a complete parametric intensity model for the three regions, the *posterior probability* is incorporated. Based on Bayes formula [12], the *posterior probability* is the probability of being in region k given that pixels q are observed, and this can be calculated as follows,

$$P(k|q) = \frac{p(q|k)P(k)}{p(q)}. \quad (2)$$

Here $p(q|k)$ is given in equation (1), $P(k)$ is the prior probability, and $p(q)$ is the pixel prior probability that is assumed

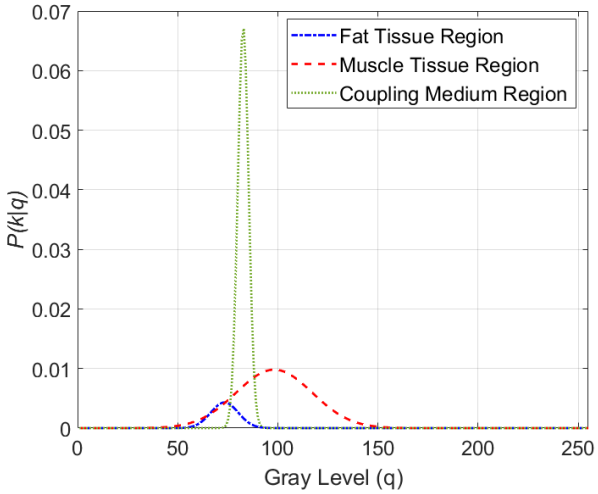

Fig. 3. The parametric intensity model for the three bulk regions in the blind reconstruction of the relative permittivity.

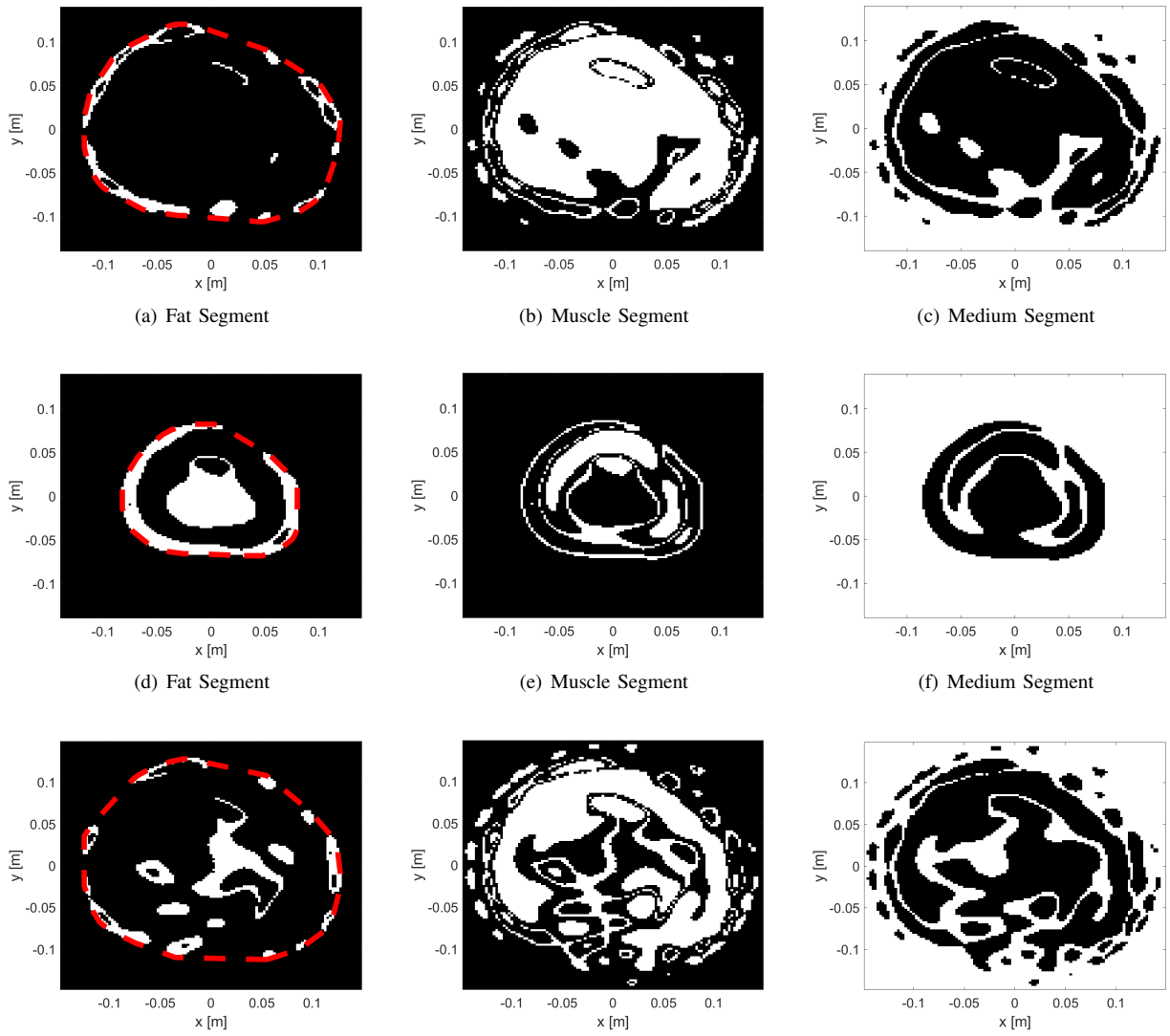

(a) Fat Segment (b) Muscle Segment (c) Medium Segment

(d) Fat Segment (e) Muscle Segment (f) Medium Segment

(g) Fat Segment (h) Muscle Segment (i) Medium Segment

Fig. 4. The Bayesian decision classifier applied on three MRI-based models: (a)-(c) Original Model, (d)-(f) Smaller Model, (g)-(i) Bigger Model.

to be 1 for all pixels. Furthermore, the prior probability, $P(k)$, is the prior knowledge of how likely a region would appear within the image. It can be calculated as follows,

$$P(k) = n_k/N. \tag{3}$$

Here n_k is the total number of pixels within extracted region k, and N is the total number of pixels within the image.

The parametric intensity model for the three regions (fat, muscle, coupling medium) is shown in Fig. 3, after applying the described procedure on the blind reconstruction shown in Fig. 1(c).

IV. Bayesian Decision Classification

After generating the parametric intensity model, it can be used to classify any blind reconstructed image into three segments using a Bayesian decision classifier. To elaborate more, given a pixel q in a reconstructed image, it is classified within region k, if and only if,

$$P(k|q) > (P(i|q)\,\&\,P(j|q)) \quad \text{where} \quad \{k \neq i \neq j\}. \tag{4}$$

Here $\{i, j, k\}$ are region indices that can be a value from $\{1, 2, 3\}$.

The result of applying the Bayesian decision classifier on Fig. 1(c) is shown in Figs. 4 (a)-(c). The figures show three classified segments from the blind reconstruction, which represent the three bulk regions in the image: the fat, muscle, and coupling medium.

For further testing, the same Bayesian classifier is applied to other blind reconstructions for two MRI-based models, which are smaller and bigger scaled versions of the original model. The results are shown in Figs. 4 (d)-(f) and (g)-(i) for the smaller and bigger models respectively.

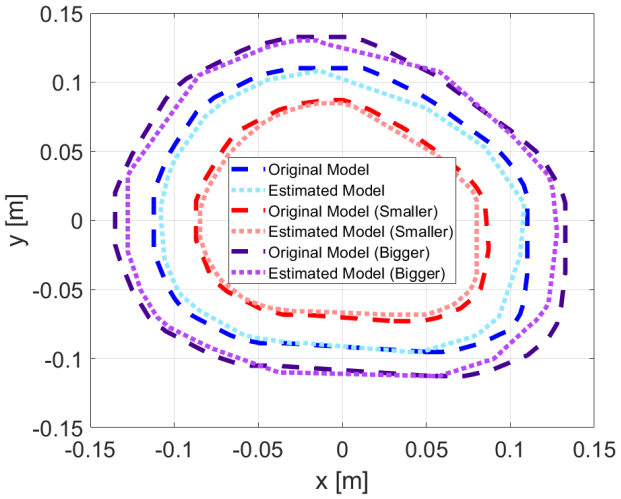

Fig. 5. The original and estimated models of the OI for the three MRI-based models

In Fig. 4 (a),(d), and (g), the red-dashed line represent the boundary of the fat layer, which can be used to estimated the leg's contour as can be represented in Fig. 5. Furthermore, the outermost boundaries are estimated by slightly extruding the fat boundaries to depict the presence of the skin layer. The L_2-norm values for the difference between the actual and estimated leg boundaries are 5.45%, 6.24%, and 4.89% for the normal, smaller, and bigger MWT images, respectively. These boundaries can be incorporated next to an inversion algorithm for improved reconstruction.

V. Conclusion

An investigation on the use of a parametric intensity model for the purpose of MWT image classification was presented in this paper. The generated intensity model was used to segment multiple reconstructed OI images using a Bayesian classifier. The results show successful extraction of the outermost boundary for three leg models, which can be incorporated as prior information in an inversion algorithm.

References

[1] M. Pastorino, *Microwave Imaging*. John Wiley & Sons, 2010, vol. 208.

[2] A. Zamani, S. Rezaeieh, K. Bialkowski, and A. Abbosh, "Boundary estimation of imaged object in microwave medical imaging using antenna resonant frequency shift," *IEEE Transactions on Antennas and Propagation*, vol. 66, no. 2, pp. 927–936, 2018.

[3] M. Omer, P. Mojabi, D. Kurrant, J. LoVetri, and E. Fear, "Proof-of-concept of the incorporation of ultrasound-derived structural information into microwave radar imaging," *IEEE Journal of Multiscale and Multiphysics Computational Techniques*, vol. 3, pp. 129–139, 2018.

[4] C. Gilmore, A. Zakaria, S. Pistorius, and J. LoVetri, "Microwave imaging of human forearms: pilot study and image enhancement," *International Journal of Biomedical Imaging*, pp. 1–17, 2013.

[5] A. Zakaria, C. Gilmore, and J. LoVetri, "Finite-element contrast source inversion method for microwave imaging," *Inverse Problems*, vol. 26, no. 11, p. 115010, 2010.

[6] A. Micheau and D. Hoa. (2017, Dec.) MRI of the lower extremity anatomy - atlas of the human body using cross-sectional imaging. Internet. [Online]. Available: https://www.imaios.com/en/e-Anatomy/Limbs/Lower-extremity-MRI

[7] C. Geuzaine and J. Remacle, "GMSH: a three-dimensional finite element mesh generator with built-in pre- and post-processing facilities," *International Journal for Numerical Method in Engineering*, pp. 1–24, 2009.

[8] Meaney, Paul M. and Fox, Colleen J. and Geimer, Shireen D. and Paulsen, Keith D., "Electrical characterization of glycerin: water mixtures: implications for use as a coupling medium in microwave tomography," *IEEE Transactions on Microwave Theory and Techniques*, vol. 65, no. 5, pp. 1471–1478, 2017.

[9] M. Alkhodari, A. Zakaria, and N. Qaddoumi, "Preliminary numerical analysis of monitoring bone density using microwave tomography," in *2018 Asia-Pacific Microwave Conference (APMC)*. IEEE, 2018, pp. 563–565.

[10] ——, "Guidelines towards a wearable microwave tomography system," in *2019 IEEE Asia-Pacific Microwave Conference (APMC)*. IEEE, 2019, pp. 1423–1425.

[11] M. Ghazal, S. Ali, M. Alkhodari, and A. El-Baz, "An Unsupervised Parametric Mixture Model for Automatic Three-Dimensional Lung Segmentation," *Lung Imaging and CADx*, p. 307, 2019.

[12] C. F. Westbury, "Bayes' rule for clinicians: an introduction," *Frontiers in Psychology*, vol. 1, p. 192, 2010.